PCCP

Can density functional theory describe multi-reference systems? Investigation of carbenes and organic biradicals†

Jürgen Gräfenstein and Dieter Cremer*

Department of Theoretical Chemistry, Göteborg University, Reutersgatan 2, S-41320 Göteborg, Sweden

Received 16th December 1999, Accepted 17th February 2000
Published on the Web 2nd May 2000

Kohn–Sham (KS) density functional theory (DFT) in its present approximate form cannot be applied to electron systems with strong multi-reference character. Various ways are discussed to develop DFT for multi-reference systems. The restricted open-shell singlet (ROSS) formalism is a modification of the conventional open-shell KS formalism, which makes a reliable, but still economical treatment of open-shell singlet biradicals possible. The complete-active-space DFT (CAS-DFT) method combines an explicit treatment of multi-configurational character with the DFT treatment of dynamic electron correlation effects. Due to the flexibility in the choice of the active space, this method is in principle appropriate for all kinds of multi-reference problems. Based on sample calculations for carbenes and organic biradicals, the advantages and limitations of ROSS-DFT and CAS-DFT are discussed. Some possibilities for future improvements of DFT methods for multi-reference problems are pointed out.

1. Introduction

Many chemically interesting processes, such as dissociation and fragmentation reactions or the formation of molecules with low-spin biradical character, involve systems with strong static electron correlation effects, the theoretical treatment of which requires multi-configurational (MC) or multi-reference (MR) methods. Such a treatment can be provided by MC self-consistent-field (MCSCF) methods such as complete-active-space SCF (CASSCF),[1] however, MCSCF (CASSCF) does not cover dynamic electron correlation effects, which are required for a quantitatively correct description. There are high-level *ab initio* methods such as multi-reference-configuration interaction (MRCI),[2,3] MR-averaged quadratic coupled-cluster (MR-AQCC)[4] or CASSCF second-order perturbation theory (CASSCF-PT2)[5] that allow a simultaneous description of static and dynamic correlation effects. However, these methods can only be applied to relatively small electron systems because of their high computational cost. This will be particularly true if, besides the energy calculation, geometry optimization and frequency calculation also have to be carried out. Two-configurational MP2 methods such as GVB-MP2[6] appear as an alternative; however, the active space they employ is often too small to cover all static electron correlation effects.

Density functional theory (DFT)[7] performs satisfactorily at low numerical expenses in those cases where dynamic correlation effects have to be covered. The Kohn–Sham (KS) formulation,[8] which is presently the basis for all applications of DFT, is, however, restricted to single-reference systems. Hence, the question arises how DFT can be generalized so that its performance and efficiency can be exploited for the description of multi-reference problems.

KS-DFT relates the ground state of the real many-particle system to a fictitious system of non-interacting electrons. The latter move in an effective potential adjusted in such a way that the reference system has the same one-electron density as the real one. The total energy of the real system is expressed as the energy of the KS reference state plus a correction accounting for electron exchange (X) and electron correlation (C) effects so that the XC energy contains all many-body effects. The XC energy is not known exactly and, therefore, has to be approximated in applications. Also, it is assumed that the reference state can be described with a single Slater determinant, which leads to the above-mentioned restriction to single-reference systems.

Replacing the effective potential in the reference state adiabatically by the real electron–electron interaction with the help of the perturbation parameter λ, reference and real state can be connected by a continuum of intermediate states (adiabatic connection scheme (ACS)[9]). In Fig. 1, the ACS is the basis for (a) classifying different types of multi-configurational states and (b) constructing DFT methods for multi-reference problems.

If the electron–electron interaction parameter λ is increased from $\lambda = 0$ (situation of the reference state with non-interacting electrons) to $\lambda = 1$ (real state), dynamic electron correlation will be continuously increased to its full magnitude. In wave function theory, this would be reflected by the fact that for increasing λ the weight of the (leading) ground state determinant Φ_0 decreases while those of excited-state determinants $\Phi_1, \Phi_2, \ldots$ increase. These changes are included in the ACSs of Fig. 1. Single- and multi-reference systems can be classified according to the dependence of the weight factors w on λ.

In the case of a conventional single-reference system [type-0, Fig. 1(a)], the ACS is characterized by two important features: (i) at $\lambda = 0$ the (multi-configurational) wave function reduces to a single-configurational, single-determinantal form represented by the KS determinant Φ_0. (ii) For all $\lambda > 0$ the wave function is dominated by Φ_0, although excited determinants $\Phi_1, \Phi_2, \ldots$ describing electron correlation effects appear in the wave function. Their weights w increase smoothly as λ

† Dedicated to Professor Reinhart Ahlrichs on the occasion of his 60th birthday.

This journal is © The Owner Societies 2000

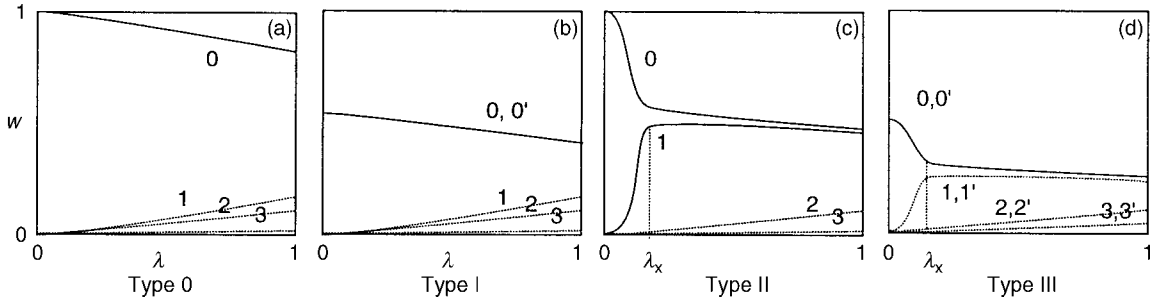

Fig. 1 Adiabatic connection schemes for type-0, type-I, type-II and type-III systems as described by the composition of the wave function in terms of KS determinants given by their weight factor w. The perturbation parameter λ gives the relative strength of electron–electron interactions, *i.e.*, $\lambda = 0$ stands for the KS reference state, $\lambda = 1$ for the real ground state. (a) Conventional single-reference, single-determinant description for closed shell systems (type-0 systems). (b) Single-reference multi-determinant description for low spin open-shell systems such as singlet biradicals (type-I systems). (c) Multi-reference description for molecules with strong static electron correlation effects (type-II systems). (d) Multi-reference, multi-determinant description for low-spin open-shell systems with strong static correlation effects (type-III systems). For (c) and (d), static correlation effects become so strong at λ_x that a single-reference description is no longer justified.

increases; however, their values remain small compared with the weight of Φ_0. The conventional KS formalism was developed and provides a reasonable description for type-0 systems that fulfill conditions (i) and (ii). However, KS theory will fail if (i) and (ii) are violated.

Fig. 1(b) presents a typical ACS for a system, for which condition (i) is not valid (type-I systems) although condition (ii) may be fulfilled. Molecules belonging to the class of type-1 systems are, for example, σ–π singlet (S) biradicals. Strictly speaking, type-I systems have no multi-reference character since they can be described by a single-configurational wave function, which, however, consists of two equivalent Slater determinants Φ_0 and Φ_0, contributing with the same weight w each, but differing with regard to the spin orientation of the electrons in the open-shell orbitals. (Generally, the reference state may consist of more than two Slater determinants, but the case of two determinants is most interesting for applications.) For type-I systems, conventional KS-DFT is wrong in principle since the two-determinantal representation cannot be replaced by a single-determinant description.

In Fig. 1(c), the ACS is shown for a system, for which condition (ii) does not hold (type-II system). Molecules with strong static electron correlation effects such as σ–σ S biradicals or dissociating molecules belong to this class. The reference state for type-II systems can still be described by a single determinant; however, as due to the strong static correlation effects the weights of some low-lying excited configurations increase rapidly with increasing λ so that from a certain λ_x ($\lambda_x < 1$) on the wave function is no longer dominated by Φ_0. For type-II systems, DFT is still valid in principle but will not work in practice since the available approximations for the XC energy are based on assumption (ii).

One could also consider the situation of a type-III system, for which both conditions (i) and (ii) are no longer valid; however, any method that can treat problems I and II appropriately can also describe a type-III molecule. Clearly, such a method has to cover both static and dynamic electron correlation effects. If one could combine the advantages of a correct MC description for the static correlation effects with those of DFT for the dynamic ones, thus yielding some MC-DFT approach, one would have a method appropriate for all problems that cannot correctly be described by conventional KS theory. While this is the maximal goal reached at the price of an additional MC calculation, partial solutions at lower cost are also possible. For example, one can focus on type-I systems and find a solution by exploiting the single configuration nature of their reference function and reformulating the problem in a single-reference framework, which leads to an efficient algorithm. Such a method, which allows the investigation of type-I systems with convenient extensions of standard KS theory, will be discussed in Section 2. In Section 3, the problems of the more general MC-DFT approach will be discussed and application examples of CAS-DFT will be presented. Finally, in Section 4 we will briefly discuss the future of DFT methods for multi-reference problems.

2. A DFT method for low-spin open-shell systems—ROSS-DFT

In Fig. 2, the electronic structures of the three lowest states of methylene (**1**), namely the $^3B_1$, $^1A_1$ and $^1B_1$ states, are schematically shown in form of simple orbital pictures. While the triplet (T) $^3B_1$ ground state represents a high-spin open-shell system and the S excited state is formally a close-shell system with type-II character, the $^1B_1$ excited state is a typical example for a low spin open-shell S (OSS) problem with type-I character, which can only be described correctly by the two-determinant approach (1):

$$\Psi = \hat{A}\{\Phi_{\text{core}}\tfrac{1}{2}[\phi_r(1)\phi_s(2) + \phi_s(1)\phi_r(2)] \times [\alpha(1)\beta(2) - \beta(2)\alpha(1)]\}. \quad (1)$$

As pointed out first by von Barth,[10] standard DFT describes the energy relationships between OSS and T states erroneously in two ways: (a) The T($M = 0$) state is predicted to have a different energy than the T($M = \pm 1$) states. (b) The T($M = 0$) state and the OSS state are predicted to be degenerate.

While error (a) is due to the limitations of the approximate XC energy functionals available, failure (b) is of principal importance: basic KS-DFT is valid only for the ground state and cannot describe the OSS state correctly. One can, however, extend DFT to be valid for the lowest state of each symmetry,[10,11] which implies that one has a separate XC energy functional for each symmetry. Taking advantage of this possibility, a KS-DFT formalism for OSS states can be derived. For this purpose, one has to construct an appropriate XC functional, which accounts for the two-determinantal character of the OSS state. This will lead to the restricted OSS-DFT (ROSS-DFT) formalism developed by Gräfenstein, Kraka and Cremer,[12] which is based on the correct treatment of OSS states and other low-spin open-shell states keeping to a large extent the usual KS formalism.

The central feature of ROSS-DFT is the construction of the XC energy functional, the form of which stipulates the corresponding KS formalism completely. The X energy of the T states can be described well within DFT by considering the T($M = 1$) state:

$$E_X^T = E_X^{DFT}[\rho_\alpha, \rho_\beta] = E_X^{DFT}[\rho_c + \rho_r + \rho_s, \rho_c], \quad (2)$$

where ρ_c, ρ_r and ρ_s are the electron densities associated with the doubly occupied space (core c), and the two open-shell

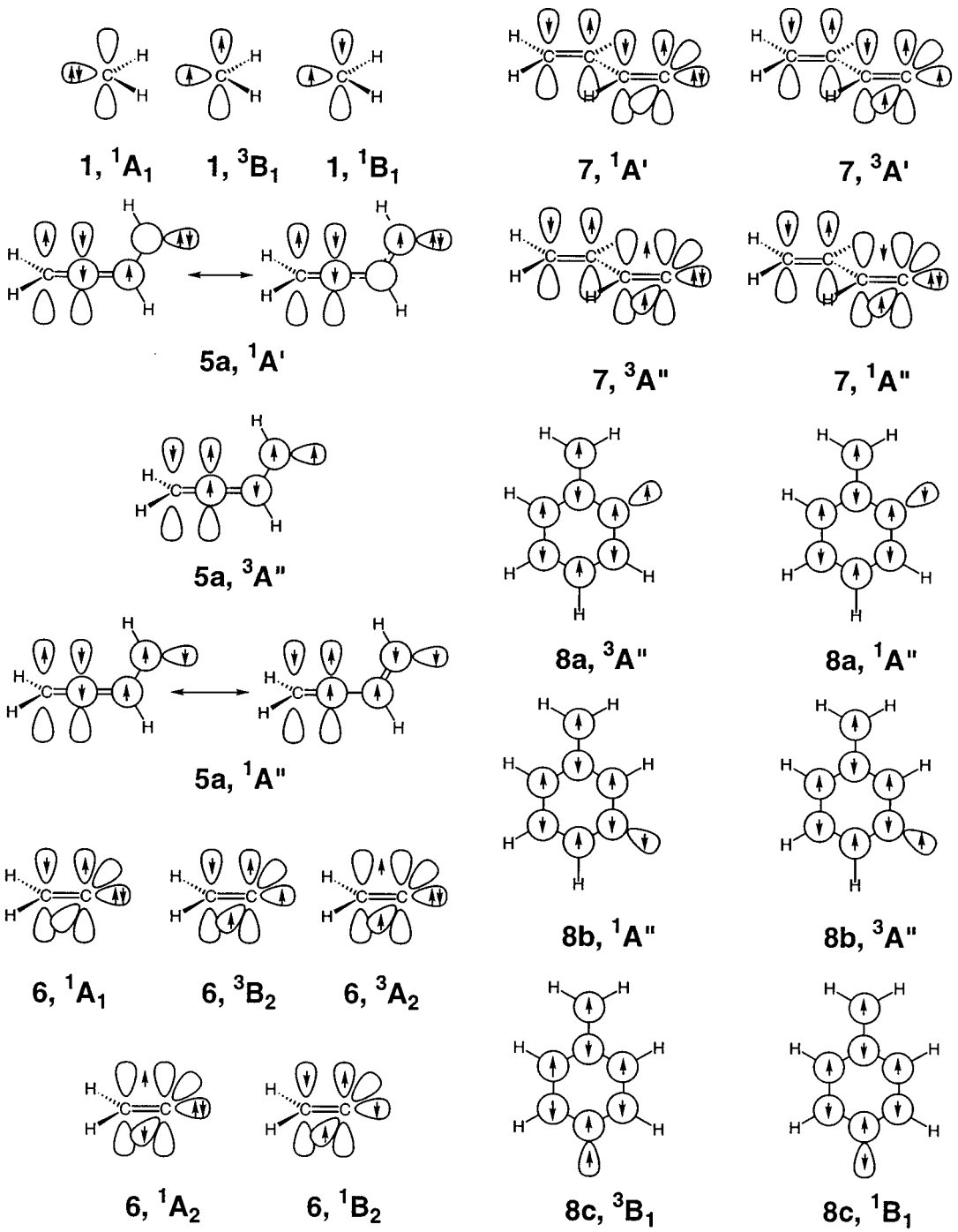

Fig. 2 Schematic representation of the lowest electronic states investigated for some of the molecules investigated in this work

orbitals ϕ_r and ϕ_s, respectively, and E_X^{DFT} is the DFT expression for the exchange energy. The difference between the X energies of T and OSS state can be found by considering the T($M = 0$) state. It is given by twice the exchange integral K_{rs} associated with ϕ_r and ϕ_s. Thus one gets as expression for the X energy of the OSS state:

$$E_X^{ROSS} = E_X^{DFT}[\rho_c + \rho_r + \rho_s, \rho_c] + 2K_{rs}. \quad (3)$$

The ROSS C energy is expressed by eqn. (4):

$$E_C^{ROSS} = E_C^{DFT}[\rho_c + \rho_r, \rho_c + \rho_s]. \quad (4)$$

Despite its simplicity, expression (4) covers important features of the electron correlation in the OSS state: (i) the electrons in the ϕ_r and ϕ_s orbitals are described as opposite-spin electrons, (ii) the correlation between the core electrons and the electrons in the ϕ_r and ϕ_s orbitals is covered correctly.

Based on the ROSS-DFT XC functional, the KS orbitals are determined in the usual way as orthonormal orbitals that minimize the total energy functional. The corresponding KS equations are derived from the requirement that the total energy must not change in first order for infinitesimal changes of the orbitals that conserve their orthonormality. The resulting formalism resembles the low-spin ROHF method.[13] Analogous to low-spin ROHF theory, the KS orbitals can be represented as eigenvectors of a segmented Fock matrix, *i.e.* a Fock matrix where elements between different kinds of orbitals (core, ϕ_r, ϕ_s, valence) are constructed in a different way. Development and implication of the ROSS-DFT method is described in more detail in ref. 12.

For the comparison of ROSS-DFT energies with energies of T or closed-shell S states, the latter must be calculated at a level of theory adequate to ROSS-DFT. This means that one should use restricted DFT (RDFT) even if the RDFT solution is externally unstable and restricted open-shell (RO) DFT for T states in contrast to the fact that generally UDFT rather

than RODFT is more appropriate for the description of high-spin open-shell states.[14] In the following, ROSS-DFT results are always referenced with regard to appropriate RODFT or RDFT calculations.

In Table 1, relative energies of the three lowest states of methylene (**1**), methylmethylene (**2**), dimethylmethylene (**3**), cyclopentylidene (**4**), allenylcarbene (**5**), vinylidene (**6**) and vinylvinylidene (**7**, see Scheme 1) are listed. All DFT calculations were done with the Becke-3 hybrid X functional (B3)[15] and the C functional of Lee, Yang and Parr (LYP).[16] Molecules **1**, **2**, and **3** were described with Dunning's cc-pVDZ, cc-pVTZ and cc-pVQZ basis sets,[17] while for the other carbenes Pople's 6-31G(d,p)[18] and 6-311 + G(d)[19] basis sets were used. All calculations were carried out with the *ab initio* packages COLOGNE 99[20] and GAUSSIAN 98.[21] DFT geometries obtained in this way are summarized in Fig. 3.

DFT predicts that **1** and **2** possess T ground states while **3** has a S ground state in line with experiment and the results of other quantum chemical investigations. The S_0–T splitting decreases from **1** (10.2 kcal mol^{-1}, Table 1) to **2** (4.1 kcal mol^{-1}) to **3** (−1.0 kcal mol^{-1}) to **4** (−9.0 kcal mol^{-1}) while the corresponding S_1–T splitting varies just by 3 kcal mol^{-1} between 28.2 (**4**) and 31.7 kcal mol^{-1} (**2**, Table 1).

Cramer and co-workers[22] discussed the performance of DFT in the case of the S_0–T splitting for **1**, **2**, and **3**. They found that BLYP, even in connection with a cc-pVDZ basis set, leads to the most reliable results while CCSD(T) splittings are 3 kcal mol^{-1}, CASSCF and CASSCF-PT2 are even 6 to 8 kcal mol^{-1} too large where the larger discrepancies are found for CASSCF-PT2 rather than CASSCF. The most accurate value for **2** was obtained at the BLYP/cc-pVQZ level of theory (3.9 kcal mol^{-1}) and for **3** at BLYP/cc-pVDZ −1.0 kcal mol^{-1}. The B3LYP/cc-pVDZ results listed in Table 1 confirm these values and clarify that the B3LYP functional performs in the same way if not even better in the case of carbenes. The calculated S_0–T splittings for **1** indicate that an increase of the basis set from cc-pVDZ to cc-pVQZ quality leads to a slight decrease from 11.1 to 10.2 kcal mol^{-1}, which has to be taken into account when considering cc-pVDZ results for **2**, **3**, and other carbenes.

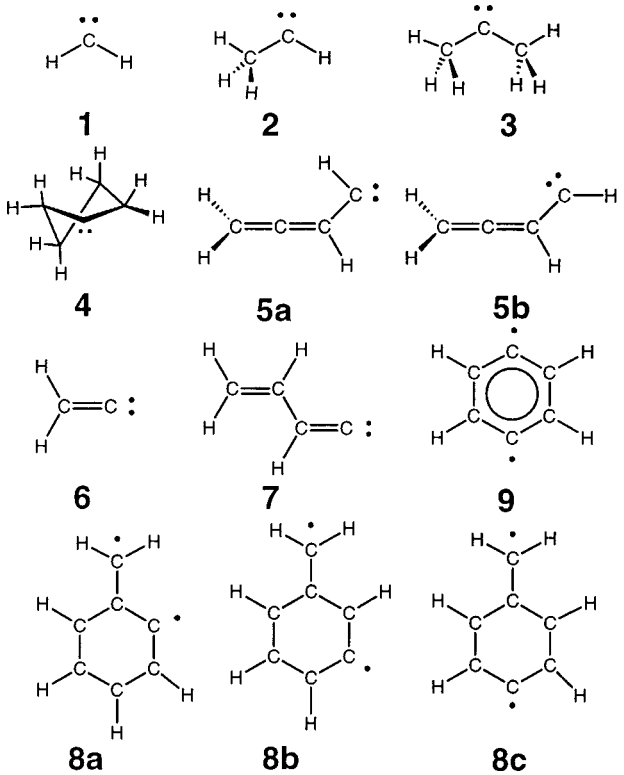

Scheme 1 Schematic representation of the structures of molecules **1**–**9**

A somewhat stronger dependence on the basis set is found for the S_1–T splitting in the case of **1**, which decreases from 33 to 29.8 kcal mol^{-1} (Table 1). These values are close to a CISD estimate (33.4 kcal mol^{-1}) given by Bauschlicher.[23] Fig. 3 shows the optimized ROSS-B3LYP geometries and geometries from ROMP2/TZ2P calculations of Andrew and co-workers[24] and experiment.[25] Noteworthy is that the ROSS value for the HCH angle of the $^1B_1$ state of **1** is 4–5° larger than the corresponding values from the CISD calculation[23] and experiment.[25b] In the $^1B_1$ state, the two single electrons are coupled and, therefore, can approach themselves and the C nucleus much closer than in the $^3B_1$ state where exchange repulsion hinders the approach of two electrons toward the nucleus at the same time. Hence, the C nucleus is more electronegative in the S_1 than in the T state, which causes a larger shift of negative charge from the H atoms to C atom. The positively charged H atoms repel each other, the HCH angle is widened, and becomes larger than in the T state. Calculations with the BLYP functional lead to a similar exaggeration of the value of the HCH angle, which suggests that the ROSS method rather than the choice of the XC functional is responsible for the angle widening. In this connection it is relevant to point out that ROSS uses a HF exchange integral K for the description of the OSS state. HF exchange is known to be larger than DFT exchange thus enhancing the difference between S_1 and T state. The electrons couple tighter and are closer to the nucleus, charge transfer from the H atoms toward the C nucleus is increased and, by this, repulsion occurs between the positively charged H atoms, which leads to an exaggeration of the HCH angle.

ROMP2/TZ2P calculations[24] lead to a S_1–T splitting of 34.6 kcal mol^{-1} while CASSCF(6,6)/cc-pVQZ predicts 40.6 kcal mol^{-1}. Even if ROSS/B3LYP somewhat underestimates the S_1–T and similarly the S_1–S_0 splitting, the comparison with experimental[26,27] and *ab initio*[23,28] values in Table 1 shows that the B3LYP description yields the most balanced overall description of the three lowest electronic states of **1**, which suggests that results for **2**, **3**, and **4** are similarly reliable.

The relative energies of the first three states of carbenes **1**–**5** can be discussed with the help of the bond separation reaction (5):

$$X\text{–}C\text{–}Y + CH_4 \rightarrow X\text{–}CH_2\text{–}Y + CH_2 \qquad (5)$$

In Table 2, calculated stabilization energies are listed.

As has been discussed before,[29] the S_0–T splitting of alkyl-substituted carbenes relative to that of **1** is reduced because of hyperconjugative stabilization of the S_0 state (stabilizing two-electron interactions involving the pseudo-π-orbital of the alkyl group and the empty pπ-orbital of the carbene C atom), but not of the T state. This interpretation is confirmed by the calculated geometries (Fig. 3), which reveal that C–C bond length of **2** is slightly shorter and the C–C–H angles significantly smaller in the S_0 than the T state. According to the bond separation energies of Table 2, methylene is stabilized by a methyl group by 15 kcal mol^{-1} and by a second methyl group by another 12 kcal mol^{-1} (totalling 27 kcal mol^{-1}) which is in line with results obtained by Bettinger and co-workers.[27]

A priori, stabilizing three-electron interactions in the T state should be much smaller; however, they can be increased by decreasing pseudo-π,π overlap,[30] which implies a widening of the C–C–H angles (Fig. 3, from 90.9 and 105.1 to 112.1 and 111.0°, respectively). Methyl stabilization accounts for only 8 and 14 kcal mol^{-1} in the T states of **2** and **3**. The ROSS geometry of the S_1 state of **2** (Fig. 3) reveals that angle-widening is even larger and that there is the possibility that stabilizing three-electron interactions are stronger in this than the T state. We calculated stabilization energies of 9.4 and 19.3 kcal mol^{-1} for **2** and **3**, respectively (Table 2). Hence, three-electron stabilization effects are slightly stronger in the

Table 1 Energies for the lowest triplet and singlet states of several carbenes[a]

Molecule	Species	Method	Basis	T^b	Sym.	E/E_h	S_0	Sym.	$\Delta E(S_0 - T)$/ kcal mol^{-1}	S_1	Sym.	$\Delta E(S_1 - T)$/ kcal mol^{-1}	$\Delta E(S_i - S_0)$/ kcal mol^{-1}	Ref.
H_2C:	**1**	ROSS-DFT	cc-pVDZ	$^3B_1$	C_{2v}	−39.15157	$^1A_1$	C_{2v}	11.1	$^1B_1$	C_{2v}	33.0	21.9	This work
			cc-pVTZ			−39.16668			10.5			30.4	19.9	This work
			cc-pVQZ			−39.16969			10.2			29.8	19.6	This work
			6-31G(d,p)			−39.15156			12.4			34.7	22.3	12
		MP2	TZ2P			−39.04703			16.3			34.6	18.3	24
		CASSCF(6,6)	cc-pVQZ			−38.97356			10.2			40.6	30.4	39
		CAS(6,6)-DFT	cc-pVQZ			−39.12321			6.6			34.8	28.2	39
		CI[b]	Large basis						9.1			33.4	24.3	23,28
		Expt.[c]							9.4					27
$H(CH_3)C$:	**2**	ROSS-DFT	cc-pVDZ	$^3A''$	C_s	−78.47754	^1A	C_1	4.1	$^1A''$	C_s	31.7	27.6	This work
$(CH_3)_2C$:	**3**	ROSS-DFT	cc-pVDZ	$^3B_1$	C_{2v}	−117.80284	^1A	C_2	−1.0	$^1B_1$	C_{2v}	29.4	30.4	This work
c-$(CH_2)_4C$:	**4**	ROSS-DFT	6-311 + G(d)	^3B	C_2	−195.25219	^1A	C_2	−9.0	^1B	C_2	28.2	37.2	This work
		UDFT	6-311 + G(d)			−195.25423			−7.7			10.8	18.5	32
		CASSCF-PT	ANO										36.6	32
$(H_2C{=}C{=}CH)HC$: (syn)	**5a**	ROSS-DFT	6-31G(d,p)	$^3A''$	C_s	−154.64162	$^1A'$	C_s	3.6	$^1A''$	C_s	16.1	12.5	This work
		UDFT	6-31G(d,p)			−154.64671	^1A	C_1	3.6			8.3	4.7	This work
$(H_2C{=}C{=}CH)HC$: (anti)	**5b**	ROSS-DFT	6-31G(d,p)	$^3A''$	C_s	−154.64105	$^1A'$	C_s	4.1	$^1A''$	C_s	14.8	10.7	This work
		UDFT	6-31G(d,p)			−154.64625	^1A	C_1	5.0			8.0	3.0	This work
$H_2C{=}C$:	**6**	ROSS-DFT	6-31G(d,p)	$^3A_2$	C_{2v}	−77.17305	$^1A_1$	C_{2v}	−56.7	$^1A_2$	C_{2v}	8.7	65.4	This work
		UDFT	6-31G(d,p)			−77.17875			−53.2			2.5	55.7	This work
		EOM-CC	ANO			−77.01724			−62.3			9.4	71.7	36
		Expt.[d]							−62.7					37
$(H_2C{=}CH){-}CH{=}C$:	**7**	ROSS-DFT	6-31G(d,p)	$^3A''$	C_s	−154.59909	$^1A'$	C_s	−42.2	$^1A''$	C_s	6.7	48.9	This work
		UDFT	6-31G(d,p)			−154.60273			−39.9			2.4	42.3	This work

[a] Absolute energies in hartrees, energy differences in kcal mol^{-1}. DFT calculations with the B3LYP functional at optimized geometries. CASSCF and CAS-DFT calculations at CASSCF(6,6)/cc-pVDZ geometries. S_0 denotes the lowest singlet state. T and S_1 possess the same electron configuration. [b] $\Delta E(S_0 - T)$ estimated by extrapolation to large basis sets, ref. 23. $\Delta E(S_0 - T)$ from SOCI + Q/ANO calculations, ref. 28. [c] T_0 value[26] converted into T_e.[27] [d] T_0 value converted into T_e using harmonic frequencies from ref. 36.

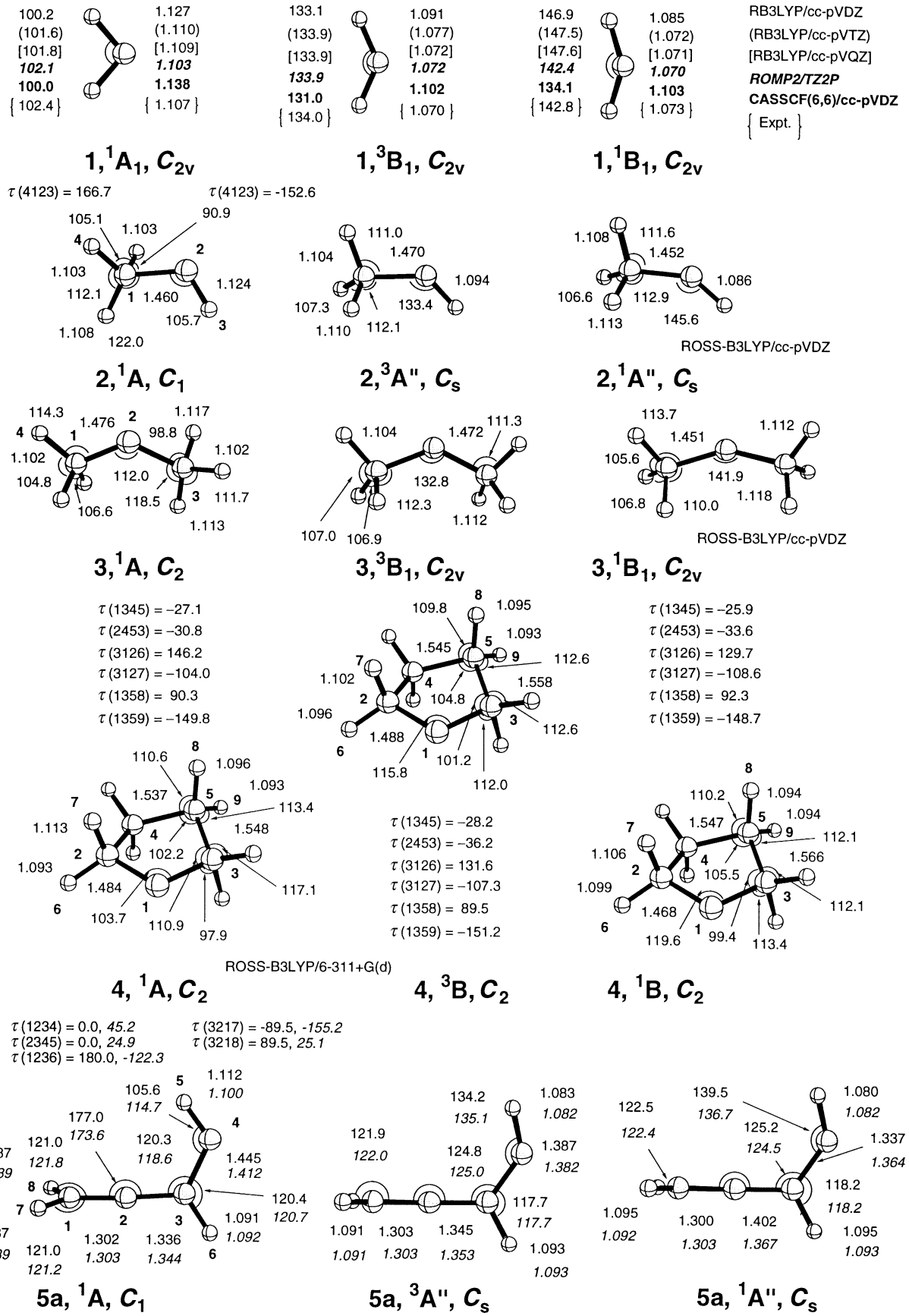

Fig. 3 Optimized geometries for molecules **1**–**9**. ROSS-B3LYP values in normal print, UB3LYP values in italic. ROMP2 geometries for **1** from ref. 24, experimental geometries for **1** from ref. 25*a* ($^1A_1$ state) and ref. 25*b* ($^3B_1$ and $^1B_1$ states), EOM-CC geometries for **6** from ref. 36.

S_0 than the T state, which is reflected by the corresponding S–T splittings listed in Table 1. Again, the electronegativity of the C atom increases in the S_1 state relative to that in the T state, which leads to a widening of the C–C–H angle and a shortening of the C–C bond where three-electron interactions (less developed in the T state) enhance this effect.

There are other effects such as steric repulsion between the alkyl groups and rehybridization at the carbene C atom,

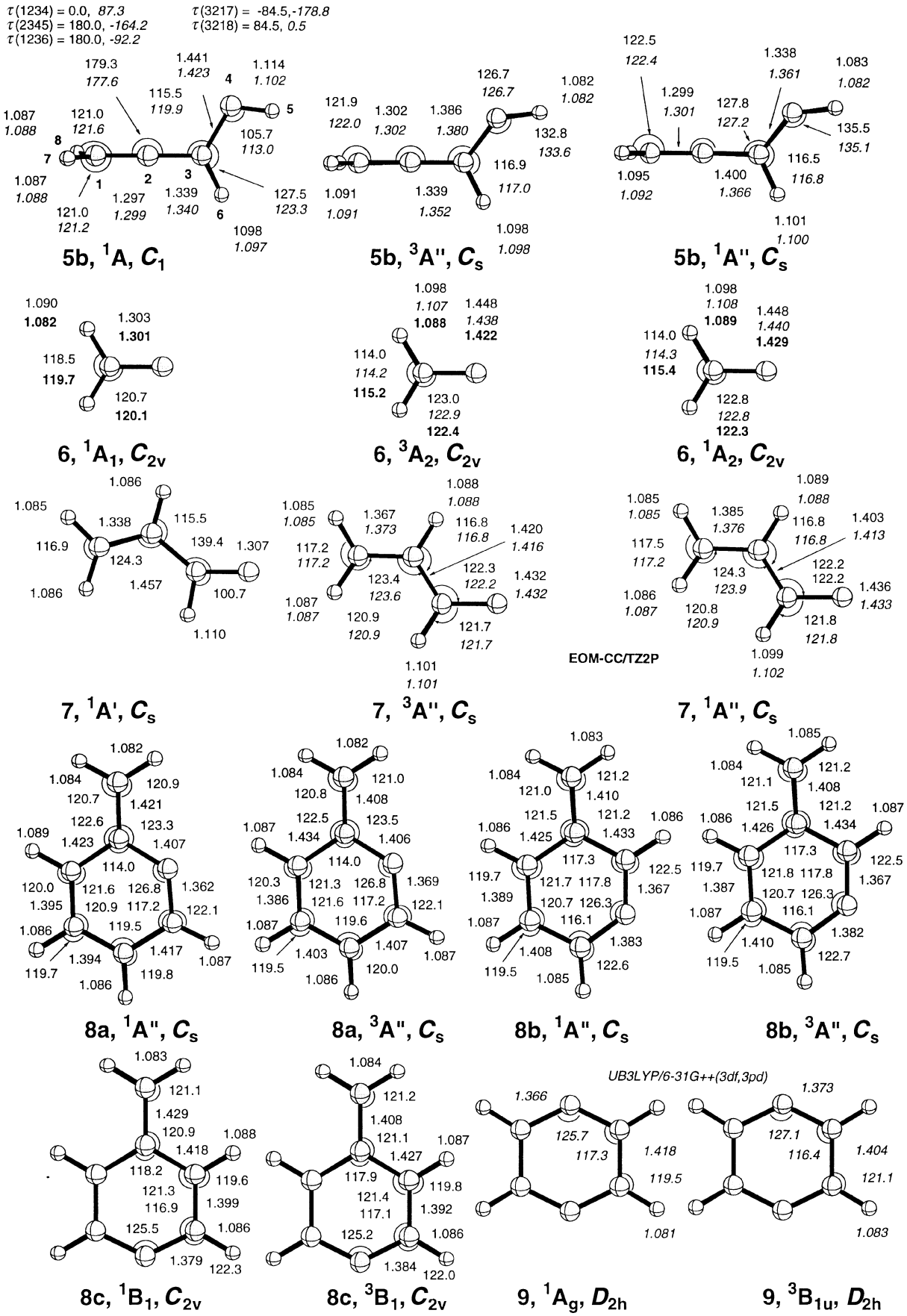

Fig. 3 Continued.

which have been extensively discussed for the S_0 and T states of carbenes by Carter and Goddard.[31] However, the observed inversion of the S_0–T splitting and the slight reduction of the S_1–S_0 splitting should predominantly be influenced by hyperconjugative stabilization of the S_0 state relative to the T state and a much smaller three-electron stabilization of the S_1 state relative to the T state.

If the carbene C atom is incorporated in a five-membered

Table 2 B3LYP bond separation energies of substituted carbenes X–C̈–Y according to reaction (5)[a]

Species	X–	Y–	Basis	T	S_0	S_1
2	CH_3–	H–	cc-pVDZ	8.2	15.2	9.4
3	CH_3–	CH_3–	cc-pVDZ	14.8	26.8	19.3
4	–C_4H_8–		6-311 + G(d)	13.5	33.0	17.1
5a	H_2C=C=CH–	H-(*syn*)	6-31G(d,p)	18.4	27.2	37.1
5b	H_2C=C=CH–	H-(*anti*)	6-31G(d,p)	18.0	26.3	38.0
6	H_2C=		6-31G(d,p)	−30.3	38.8	−4.3
7	CH_2=CH–CH=		6-31G(d,p)	−18.9	35.7	9.1

[a] Absolute energies in hartrees, energy differences in kcal mol^{-1}. Positive (negative) energies denote a (de)stabilization of carbene X–C̈–Y relative to H_2C:.

ring thus yielding cyclopentylidene (**4**, Scheme 1), the S_0 state is stabilized even more strongly than in **3**. Recently, Xu and co-workers[32] investigated the possible mechanisms for formation and cleavage of **4** both theoretically and experimentally. Since **4** was generated in a highly exothermic process, one possible reaction path included the formation of the OSS ^{1}B state of **4**. Xu and co-workers calculated the relative energy of the three lowest states of **4** to be 7.7 (T state above S_0) and 18.5 kcal mol^{-1} (S_1 state above S_0 state) at UB3LYP/6-311 + G(d) where no considerations of the type-I character of the S_1 state and the problems thus involved in a DFT calculation were made. However, CASSCF(12,12)-PT2/ANO calculations at the UB3LYP geometry were carried out to correct the UDFT result to 36.6 kcal mol^{-1}. We optimized the geometry of **4**-S_1 at the ROSS-B3LYP/6-311G + (d) level of theory and obtained an excitation energy of 37.2 kcal mol^{-1}, *i.e.* just 0.6 kcal mol^{-1} off the CASSCF-PT2 value (Table 1). The S_1–T splitting at ROSS-B3LYP/6-311G + (d) is 28.2 kcal mol^{-1} compared with 10.8 kcal mol^{-1} at UDFT.

Carbene **4** in its S_0 ground state is more stabilized than **3** (33 *vs.* 27 kcal mol^{-1}, Table 2) although stabilization energies in T and S_1 states are similar to those calculated for dimethylcarbene **3**. Different electronic and steric effects are responsible for these trends. Bond eclipsing is reduced in **4** relative to cyclopentane, which is reflected by the S_0 stabilization energy (cyclopentane is the reference molecule X–CH_2–Y in reaction 5). Prerequisite for the reduction of eclipsing strain is a relatively strong puckering of the five-membered ring as measured by the ring puckering amplitude q_2 [33] (reference value for cyclopentane: 0.397 Å). On the other hand, hyperconjugative stabilization requires a flat five-membered ring to guarantee sufficient overlap between pseudo-π and π orbitals. Accordingly, **4**-S_0 is least puckered ($q_2 = 0.317$ Å). Three-electron stabilization requires a reduction of overlap and strong puckering ($q_2 = 0.351$ and 0.325 Å for the T and S_1 states, respectively; Fig. 3), which requires an increase in strain since the relatively large (H_2)C–C–C(H_2) angle associated with the $\sigma^2\pi^1$ electron configuration of T and S_1 state has to be reduced with increasing puckering. Hence, stabilizing and destabilizing effects are balanced in the case of the T and S_1 state while for the S_0 state hyperconjugative stabilization is augmented by a decrease in eclipsing strain.

Conjugated carbenes such as vinyl or allenyl carbene **5** (Scheme 1) are strongly stabilized in all states. Since carbene **5** was recently spectroscopically identified by low temperature matrix isolation studies, we calculated the three lowest states of this molecule, which can exist in a *syn* form **5a** or an *anti* form **5b** (Scheme 1, Fig. 3).[34] Calculations at the DFT level show that both **5a** and **5b** possess a T ground state while the S_0 state is just 4 kcal mol^{-1} above the ground state (Table 1) similarly as in the case of **2**. As shown in Fig. 2, delocalization of the π electrons of the adjacent allene double bond into the empty pπ orbital at the carbene C is rather limited in the S_0 state since it leads to a weakening of the double bond and, therefore, the stabilization of the S_0 state relative to the T state is moderate and comparable to a hyperconjugative interaction.

ROSS-B3LYP calculations reveal that the S_1 state is strongly stabilized (by 18.6 and 19.9 kcal mol^{-1}, Table 1) relative to the lower states, which is also reflected by the stabilization energies listed in Table 2. Hence, the S_1 state is just 12.5 and 10.7 kcal mol^{-1} above the S_0 state for **5a** and **5b**, respectively. An investigation of calculated geometries and electronic structures reveals that **5** in its S_1 state actually corresponds to a biradical (see Fig. 2) rather than a carbene and is best described as a butadienediyl biradical (two H atoms at C1 and C3 are abstracted) that is rotated at the allene end into a 90° conformation. Accordingly, it is not surprising that both the *syn* and the *anti* form of **4**-S_1 turn out to be a transition state for CH_2 rotation. If one uses buta-1,3-diene rather than methylallene [$\Delta H_f^0(298) = 26.3$ and 38.8 kcal mol^{-1}, respectively[35]] as a suitable reference in reaction (5), the stabilization energy will be reduced from 37 to 24 kcal mol^{-1}, which is in line with the stabilization energies calculated for the other carbenes of Table 1.

The strongest interactions between carbene C and an adjacent π system can be expected for vinylidenes **6** and **7** (Scheme 1). In distinction to the σ,π biradical states of **1**, the lowest OSS state of **6** corresponds to a π,π biradical where one π orbital is in-plane, the other out-of-plane. For the excited S cases, the exchange interaction in the $(\cdots 1b_1^1 2b_2^1)$ electron configuration of the $^1A_2$ state is lower than in the $(\cdots 5a_1^1 2b_2^1)$ configuration of the $^1B_2$ state. As a consequence, **6**($^1A_2$) is lower in energy than **6**($^1B_2$); also, the $^1A_2$–$^3A_2$ splitting in **6** is considerably smaller than the $^1B_1$–$^3B_1$ splitting in **1**. For the T cases, however, $^3B_2$ is lower in energy than $^3A_2$. The ground state of **6** is a closed-shell ($^1A_1$) S. Equation-of-motion coupled-cluster (EOM-CC) calculations by Stanton and Gauss[36] with a large ANO basis set predict excitation energies T_e for the $^3B_2$, $^3A_2$, and $^1A_2$ states to be 46.5, 62.3 and 71.7 kcal mol^{-1}, respectively, *i.e.* the $^1A_2$–$^3A_2$ splitting is calculated to be 9.4 kcal mol^{-1}. ROSS-B3LYP/6-31G(d,p) calculations lead to a $^1A_2$–$^3A_2$ splitting of 8.7 kcal mol^{-1} as compared with 2.5 kcal mol^{-1} at the UB3LYP/6-31G(d,p) level of theory, which means that ROSS-B3LYP in distinction to UB3LYP describes the relative energy of the $^3A_2$ and $^1A_2$ states correctly. However, ROSS-B3LYP yields too low an energy of the $^{1,3}A_2$ states relative to the ground state. The ROB3LYP excitation energy of the $^3A_2$ state is 56.7 kcal mol^{-1}, *i.e.* 5.6 kcal mol^{-1} below the EOM-CC value and 6.0 kcal mol^{-1} below the experimental value of 62.7 kcal mol^{-1} (ref. 37) (photodetachment measurements, extrapolated to T_e with the harmonic vibration frequencies from ref. 36). Obviously the DFT description exaggerates electron delocalization that results when the molecule is excited from the ground state to one of the $^{1,3}A_2$ states. One can expect that the accuracy of the DFT results can be improved by an approach that corrects this exaggeration, *e.g.* by including self-interaction corrections.[38]

Vinylvinylidene (**7**) plays an important role as an interme-

diate on the C_4H_4 potential energy surface.[34] Its lowest S and T states are similarly ordered as the corresponding vinylidene states (Fig. 2 and Table 1), *i.e.* the ground state is a S state with a σ^2 electron configuration, the first and second excited T states ($^3A'$ and $^3A''$) correspond to the $^3B_2$ and $^3A_2$ states of **6**, and the following $^1A''$ state to the first OSS state of **6**. ROSS-B3LYP/6-31G(d,p) predicts a decrease in the S_1–S_0 splitting (48.9 kcal mol^{-1}, Table 1) by 14.5 kcal mol^{-1} relative to the corresponding excitation energy of **6** where these values result from the fact that in the S_1 state a π bond is broken (energy loss: *ca.* 65 kcal mol^{-1}), which in the case of **7** is partially compensated by establishing an allyl system (Fig. 2).

While ROSS-DFT is rather reliable in the case of the OSS states of carbenes, care has to be taken when it is applied to OSS states of organic biradicals with considerable spin polarization effects. Although ROSS may lead to reasonable geometries in these cases it may predict S–T splittings wrongly. This has to do with the fact that these molecules belong to type-III systems, which are better described with a genuine MC method combined with DFT.

3. The combination of MC methods and DFT: the CAS-DFT method

Static electron correlation effects can be described routinely by a MC wave function with a moderately-sized active space. The available methods for a simultaneous inclusion of static and dynamic correlation effects such as CASSCF-PT2,[5] MR-ACPF[2] or MR-AQCC,[4] however, are generally not feasible for larger molecular systems since the combination of MC or MR methods with perturbation or coupled cluster theory leads to complicated and very costly calculation procedures. Computational cost would be considerably improved if one could combine a MC or MR method with DFT, thus covering both static and a relatively high amount of dynamic electron correlation effect. Choosing CASSCF[1] as a suitable method for constructing the MC wave function one would obtain CAS-DFT as a more generally applicable DFT method.[39] CAS-DFT should be able to handle type-III systems and, by this, also all genuine type-I or type-II systems.

The development of CAS-DFT implies more than the simple addition of CASSCF and KS-DFT. A number of problems such as the proper choice of input quantities (spin densities, total density, *etc.*), the avoidance of a double-counting of electron correlation effects, the correct distinction between core and active space correlation effects at the DFT level, a balanced treatment of singly and doubly occupied CAS orbital or the best choice of the DFT correlation functional. We will discuss in the following these problems one after the other to establish the theoretical foundation of CAS-DFT.

3.1. Choice of the input densities for the DFT correlation energy functional

The use of spin densities ρ_α and ρ_β in CAS-DFT will lead to similar errors in the description of state multiplets as discussed in Section 2 for conventional KS-DFT. Perdew and co-workers[40] pointed out that one can overcome these problems by using the total density $\rho(\boldsymbol{r})$ and the on-top pair density $P(\boldsymbol{r},\boldsymbol{r})$ as input quantities for the correlation functional. The on-top pair density can be derived from the pair density $P(\boldsymbol{r},\boldsymbol{r}')$ by setting $\boldsymbol{r} = \boldsymbol{r}'$ so that $P(\boldsymbol{r},\boldsymbol{r})$ gives the probability of finding two electrons at the same position $\boldsymbol{r}$. Being a two-particle quantity, $P(\boldsymbol{r},\boldsymbol{r})$ can distinguish between states with different multiplicity and, in distribution to ρ_α, ρ_β, the on-top density is identical for the components of a state multiplet such as T($M = -1$), T($M = 0$), and T($M = 1$).

The quantities $\rho(\boldsymbol{r})$ and $P(\boldsymbol{r},\boldsymbol{r})$ do not fit directly into the usual DFT correlation energy functionals, which have spin densities ρ_α and ρ_β as arguments. Thus, ρ_α, ρ_β, $P(\boldsymbol{r},\boldsymbol{r})$ have to be transformed according to

$$\rho_{\alpha,\beta}(\boldsymbol{r}) \rightarrow \frac{\rho(\boldsymbol{r})}{2} \pm \sqrt{\left(\frac{\rho(\boldsymbol{r})}{2}\right)^2 - \frac{P(\boldsymbol{r},\boldsymbol{r})}{2}}. \quad (6)$$

where the plus sign corresponds to the α and the minus sign to the β-spin density.

3.2. The double counting of electron correlation effects

As the active space for the CAS wave function is increased, this wave function will cover not only static correlation effects but also an increasing part of the dynamic correlation effects already contained in the DFT description. Hence, a simple combination of the DFT correlation energy and the CASSCF energy leads to an exaggeration of the molecule stability.

Expressions for the DFT correlation energy are usually derived using the homogeneous electron gas (HEG) as basis, and the HEG can also be used to investigate double-counting of dynamic electron correlation at the CAS-DFT level. The orbitals used to describe the energy of the HEG are plane waves. In the HF ground state of the HEG, all orbitals are doubly occupied up to the Fermi level ε_F, which depends on the density ρ of the HEG; orbitals above ε_F are unoccupied.

Electron correlation effects in the HEG can be described similarly as for a molecule with an inhomogeneous electron density by constructing a molecular wave function from ground and excited configurations where the latter result by existing electrons from occupied into unoccupied orbitals. These excitations comprise all occupied and all unoccupied orbitals. A CASSCF description of the HEG is limited in so far as it covers only those excitations for which all active orbitals lie between energies $\varepsilon_{core} < \varepsilon_F \leqslant \varepsilon_{act}$. Orbitals with $\varepsilon \leqslant \varepsilon_{core}$ are inactive (core) orbitals and are kept doubly occupied in all excited configurations while virtual orbitals with $\varepsilon > \varepsilon_{act}$ are kept always unoccupied.

The energy ε_{core} is a measure for the size of the inactive space and ε_{act} a measure for that of the active space. Energies ε_{core} and ε_{act}, in turn, are associated with densities ρ_{core} and ρ_{act}, which would result if all orbitals up to ε_{core} and all orbitals up to ε_{act}, respectively, were doubly occupied, *i.e.*, $0 \leqslant \rho_{core} \leqslant \rho \leqslant \rho_{act}$. The CASSCF description will yield a correlation energy $\varepsilon_c^{hom,\,CASSCF}(\rho;\ \rho_{core},\ \rho_{act}) < \varepsilon_c^{hom}(\rho)$, which for a given ρ increases with increasing ρ_{act} and decreases with increasing ρ_{core}. In the HEG, there are no static correlation effects, *i.e.* the correlation energy covered by $\varepsilon_c^{hom,\,CASSCF}(\rho;\ \rho_{core},\ \rho_{act})$ is exclusively due to dynamic electron correlation effects and, therefore, has to be deduced from the DFT correlation energy of a CAS-DFT description. The CAS-DFT correlation energy per particle, $\varepsilon_c^{hom,CAS\text{-}DFT}(\rho;\ \rho_{core},\ \rho_{act})$, is given by the difference

$$\begin{aligned}\varepsilon_c^{hom,\,CAS\text{-}DFT}&(\rho;\ \rho_{core},\ \rho_{act})\\ &= \varepsilon_c^{hom}(\rho) - \varepsilon_c^{hom,\,CASSCF}(\rho;\ \rho_{cor},\ \rho_{act}),\\ &= [1 - f(\rho;\ \rho_{core},\ \rho_{act})]\varepsilon_c^{hom}(\rho) \quad (7)\end{aligned}$$

where the scaling factor f ($0 \leqslant f \leqslant 1$) gives the portion of dynamic electron correlation covered by the CASSCF approach:

$$f(\rho;\ \rho_{core},\ \rho_{act}) = \frac{\varepsilon_c^{hom,\,CASSCF}(\rho;\ \rho_{core},\ \rho_{act})}{\varepsilon_c^{hom}(\rho)}. \quad (8)$$

It was realized early that the avoidance of a double-counting of dynamic correlation effects is crucial for the appropriate formulation of an MC-DFT method, and several solutions to this problem were suggested in the literature.[41–45] A promising starting point is the approach by Savin[46] and Miehlich and co-workers,[47] which rests upon the analysis of the HEG given above. The DFT correlation energy in this

Table 3 B3LYP energies of the lowest singlet and triplet states of α,*n*-didehydrotoluene ($n = 2, 3, 4$) and (1,4)-didehydrobenzene[a]

Species	Method	T	Sym	E/E_h	S	Sym	ΔE(S − T)/ kcal mol^{-1}	Ref.
8a	ROSS-DFT	$^3A''$	C_s	−270.233 70	$^1A''$	C_s	3.9	This work
	CASSCF(8,8)			−268.559 25			7.6	This work
	CAS(8,8)-DFT			−270.042 61			6.9	This work
	DDCI2						6.4	53
8b	ROSS-DFT	$^3A''$	C_s	−270.233 35	$^1A''$	C_s	0.8	This work
	CASSCF(8,8)			−268.554 70			−3.0	This work
	CAS(8,8)-DFT			−270.039 09			−2.6	This work
	DDCI2						−2.0	53
8c	ROSS-DFT	$^3B_1$	C_{2v}	−270.233 21	$^1B_1$	C_{2v}	3.9	This work
	CASSCF(8,8)			−268.558 84			8.1	This work
	CAS(8,8)-DFT			−270.042 56			7.5	This work
	DDCI2						6.8	53
9	CASSCF(8,8)	$^1A_{1g}$	D_{2h}	−229.486 41	$^3B_{1u}$	D_{2h}	2.4	This work
	CAS(8,8)-DFT			−230.709 04			2.5	This work
	Expt.[b]						3.5 ± 0.5	56

[a] Absolute energies in hartrees, energy differences in kcal mol^{-1}. DFT calculations with ROSS-B3LYP/6-31G(d,p) at optimized geometries. CASSCF and CAS-DFT calculations with a 6-31G(d,p) basis set at ROSS-B3LYP/6-31G(d,p) geometries. [b] T_0 value from ref. 56 converted into T_e.[57]

approach is equal to

$$E_c^{\text{CAS-DFT}} = \int d^3r[1 - f(\rho; \rho_{\text{core}}, \rho_{\text{act}})]\varepsilon_c[\rho, P]|_r, \quad (9)$$

i.e. the amount of dynamic correlation energy covered by the CAS wave function is estimated locally by the factor *f*, which is based on the local values for ρ_{core} and ρ_{act}. The function $f(\rho; \rho_{\text{core}}, \rho_{\text{act}})$ cannot be determined exactly since a CASSCF calculation for the HEG is not feasible. Savin[46] found an approximation for *f* by reanalyzing the calculation of the correlation energy for the HEG by Gell-Mann and Brueckner.[48] Later, the numerical results of Savin's work were parametrized by Miehlich and co-workers.[47] This approximation, however, is limited to the special case $\rho_{\text{core}} = 0$, *i.e.* all occupied orbitals are assumed to be active. This is not adequate for real CASSCF calculations, where one attempts to keep the inactive space as large as possible to reduce computational costs. Hence, use of Savin's approximation leads to the third problem.

3.3 Distinction between core and active space contributions to the dynamic correlation energy

The scaling of the dynamic correlation energy to avoid a double-counting of correlation effects has to be generalized in the case of a ρ_{core} density associated with an active space of finite size. In previous work,[39] we derived a core correction that is based on the expression for *f* by Savin[46] and Miehlich and coworkers[47] and an analysis of the correlation treatment for the core electrons.

For a CASSCF calculation without any DFT corrections, correlation effects of the core electrons are suppressed completely. If a DFT correction term without any scaling (*i.e.* $f = 1$) is added, this correction comprises all correlation effects of the core electrons. The scaling factor *f* eliminates all contributions to the DFT correlation energy that are due to excitations into the weakly populated active orbitals. This is correct for excitations from the strongly occupied active orbitals, which are contained in the CASSCF wave function, but inconsistent for excitations from the core orbitals. Therefore, an extra term for core correlation effects is added, which is based on the core correlation energy $\varepsilon_c[\rho_{\text{core}}, P_{\text{core}}]$ where ρ_{core} and P_{core} are the density and on-top pair density of the core electrons. The energy ε_c covers excitations from the core orbitals into (a) strongly populated active orbitals, (b) weakly populated active orbitals, and (c) virtual orbitals. Only contribution (b) should appear in the correction term. Contributions (a) and (c) can be suppressed by multiplying $\varepsilon_c[\rho_{\text{core}}, P_{\text{core}}]$ with a new scaling factor

$$f_{\text{core}}(\rho; \rho_{\text{core}}, \rho_{\text{act}}) = f(\rho_{\text{core}}; 0, \rho) - f(\rho_{\text{core}}; 0, \rho_{\text{act}}), \quad (10)$$

where the first term in the difference corresponds to a situation in which electrons are excited from the doubly occupied core orbitals into the weakly occupied active orbitals (thus leading to the real density ρ) and the second term to that in which electrons are excited from the core orbitals to both the weakly and strongly occupied active space orbitals. The total correction term is found by integrating $\varepsilon_c[\rho_{\text{core}}; P_{\text{core}}]f_{\text{core}}(\rho; \rho_{\text{core}}, \rho_{\text{act}})$ over total space, thus leading to the corrected expression (11) for $E_c^{\text{CAS-DFT}}$:

$$E_c^{\text{CAS-DFT}} = \int d^3r[1 - f(\rho; 0, \rho_{\text{act}})]\varepsilon_c[\rho, P]|_r + \int d^3r[f(\rho_{\text{core}}; 0, \rho) - f(\rho_{\text{core}}; 0, \rho_{\text{act}})] \times \varepsilon_c[\rho_{\text{core}}, P_{\text{core}}]|_r. \quad (11)$$

3.4. Choice of the correction functional for CAS-DFT

Local-density-approximation (LDA) functionals overestimate the correlation energy considerably and, therefore, a gradient-corrected functional has to be used.[47] The Lee–Yang–Parr (LYP) functional[16] is a good choice because (i) it is successfully used in many DFT applications and (ii) it is rooted in a problem similar to the present one (calculation of the correlation energy for a SCF wave function). However, the LYP functional has been derived from the Colle–Salvetti (CS) functional,[49] which has just $\rho(r)$ and $P(r,r')$ as input quantities. Thus, we can simplify CAS-DFT by avoiding transformation (6) and using the CS functional directly. As test calculations show, this influences the results only a little.

CAS-DFT was developed,[39] implemented into the COLOGNE 99 package,[20] and applied to carbenes and some interesting organic biradicals. For **1**, CAS(6,6)-DFT/cc-pVQZ calculations yield a $^1B_1$–$^3B_1$ splitting of 34.8 kcal mol^{-1}, as compared with 40.6 kcal mol^{-1} at the CASSCF(6,6)/cc-pVQZ level (Table 1). Clearly, the CAS-DFT description accounts for relevant dynamic correlation effects that are missing for CASSCF. For the $^1A_1$–$^3B_1$ splitting, CASSCF and CAS-DFT yield 10.2 and 6.6 kcal mol^{-1}, respectively. The DFT corrections account for the stronger dynamic correlation effects in the $^1A_1$ state (one electron pair more) relative to the $^3B_1$ state but exaggerate this effect, thus underestimating the S_0–T split-

ting by 2.8 kcal mol^{-1}. As is discussed in ref. 39 in more detail, the approximation used for f systematically overestimates the amount of dynamic correlation contained in the CASSCF wave function in particular for a closed shell system such as the state $^1A_1$ of **1** and, consequently, underestimates the correlation energy to be covered by DFT, resulting in a too high total energy, *e.g.* for the $^1A_1$ state. Errors compensate each other when closed (open) shell systems are compared with other closed (open) shell systems, which is the reason for the balanced description of the $^1B_1$–$^3B_1$ splitting in **1**, but they are responsible for the underestimation of the $^1A_1$–$^3B_1$ splitting in **1**. Work is in progress to improve the scaling factor f in the way that it becomes more sensitive to the differences in correlation effects for closed and open-shell systems thus correcting present shortcomings of CAS-DFT.

Table 3 lists CASSCF/6-31G(d,p) and CAS-DFT/6-31G(d,p) energies for α,2-didehydrotoluene (**8a**), α,3-didehydrotoluene (**8b**), and α,4-didehydrotoluene (**8c**, see Scheme 1), which are interesting biradical intermediates in the Myers cyclization of eneyne-allenes,[50] which is known to be the key step in the *in vivo* action of neocarzinostatin.[51] ROSS, CASSCF, and CAS-DFT calculations were done at ROSS-B3LYP geometries where the CAS description used an (8,8) active space including the σ open-shell orbital and the seven π orbitals. S-Biradicals **8** are typical type-III systems possessing both type-I and type-II character since they represent OSS states with strong additional static correlation effects. The lowest S and T state of **8** are known to be close in energy where the actual order of states depends on spin polarization effects. Applying the intraatomic Hund rule, one can easily show that **8a** and **8c** should possess a T ground state and **8b** a S ground state (see Fig. 4).

High-level *ab initio* calculations are in line with these predictions in so far as for **8b** the lowest T state is calculated to be 1 to 3 kcal mol^{-1} above the OSS state while for the isomers **8a** and **8c** the T states are found to be 4–8 kcal mol^{-1} below the S states.[52,53] There are no measured values for the S–T splitting in **8b** and **8c**; however, experimental evidence suggests that **8b** has an OSS ground state and a S–T splitting between 0 and 5 kcal mol^{-}.[54]

Recently, Cabrero and co-workers[53] determined the vertical S–T splitting for **8a**, **8b**, and **8c** by difference-dedicated CI (DDCI2)[55] calculations and estimated that the vertical S–T splittings should differ from the adiabatic ones by at most 0.1 kcal mol^{-1}. The CAS-DFT values listed in Table 3 agree with the DDCI2 values within 1 kcal mol^{-1} while the corresponding CASSCF values always slightly exaggerate the absolute S–T splittings.

ROSS-B3LYP/6-31G(d,p) calculations for **8a**, **8b**, and **8c** yield reasonable geometries for the S and T states. The corresponding ROSS energies reflect correctly that the S state of **8b** is more stable relative to the corresponding T state than it is the case for **8a** and **8c**. However, they predict for **8b** a T rather than a S ground state with an energy splitting of 0.8 kcal mol^{-1} (Table 3). The treatment of S–T splittings with ROSS-DFT focuses (i) on the different exchange interaction between the unpaired electrons and (ii) the resulting differences in dynamic correlation effects between these electrons in the T and S states. In many cases, these effects dominate the S–T splitting thus leading to a T ground state. For **8b**, the exchange interaction between the electrons in the ϕ_r and ϕ_s orbitals is small ($K_{rs} = 0.4$ kcal mol^{-1} at the ROSS-B3LYP/6-31G(d,p) level), and the S–T splitting is dominated by static correlation effects in the π electron system, *i.e.*, **8b** combines features of a type-I and type-II system. The correlation mechanism can be understood by considering the spin-resolved natural orbitals of the CASSCF calculation.[52]

Fig. 4 reveals that, if the electron in ϕ_r of **8b** has α spin, a surplus of β spin density results at the site of ϕ_s. This implies an increase of exchange energy in the T state, *i.e.* when the electron in the ϕ_s orbital has α spin, and a decrease of exchange energy in the S state. For **8b**, this mechanism leads to a stabilization of the S state [Figs. 4(a) and 4(b)] while for **8a** and **8c** [Figs. 4(c) and 4(d)] the T state is stabilized. Since ROSS-DFT uses identical α and β orbitals in the doubly-occupied space, it is blind for these spin-polarization effects and, accordingly, predicts a T ground state for **8b** and smaller S–T splittings for **8a** and **8c**. An apparent solution is to reformulate ROSS-DFT in a spin-unrestricted fashion. However, such a formulation would not allow one to properly distinguish between core orbitals on the one hand and the singly occupied ϕ_r and ϕ_s orbitals on the other hand, thus it could not describe the OSS system properly.

para-Didehydrobenzene (**9**, Scheme 1) is an example for a type-II system, which also cannot be described by ROSS-DFT because of static electron correlation effects. We calculated the adiabatic S–T splitting of **9** with CASSCF and CAS-DFT using an (8,8) active space comprising the two open-shell σ orbitals associated with the two single electrons and the six π orbitals of the benzene system. Biradical **9** is known to possess a S ground state (3.5 kcal mol^{-1} below the T state) as the result of through-bond interactions between the single electrons at C1 and C4.[56] For a recent review, see ref. 57.

At the CASSCF level, the S ground state is 2.4 kcal mol^{-1} below the T state (Fig. 3, Table 3), *i.e.* the state correlation effects of the two open-shell σ electrons and the π system are described reasonably. The inclusion of DFT corrections increase the S–T splitting by just 0.1 kcal mol^{-1}, *i.e.* CAS-DFT yields nearly identical dynamic correlation effects in the S and T states. The result is in line with other *ab initio* calculations.[58]

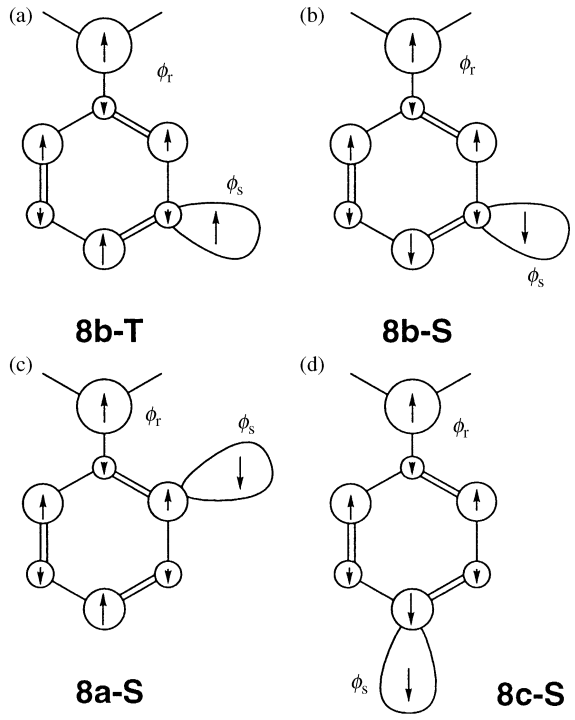

Fig. 4 Spin-resolved natural orbits for the (a) T and (b) S states of α-3-didehydrotoluene (**8b**), (c) the S state of α-3-didehydrotoluene **8a**, and (d) the S state of α-4-didehydrotoluene (**8c**). See text for a detailed explanation.

4. Conclusions and outlook

Two approaches to employ DFT for the treatment of multi-reference problems are discussed in this work. The ROSS-DFT method extends the KS formalism to the case of

low-spin open-shell problems. ROSS provides a computationally economical investigation of reactions involving such biradical states since it leads to an efficient description of the S biradical state itself and, in addition, is comparable to RDFT and RODFT results for closed- and high-spin open-shell systems occurring in a given reaction system (for a systematic application of ROSS, see, *e.g.*, ref. 34). Results presented in this work for a number of carbenes demonstrate that ROSS-DFT gives an adequate description of OSS states in cases where interactions between the two open-shell electrons are strong.

The extension of DFT beyond its original realm is an active field, and several DFT XC functionals for type-I systems were suggested in the literature at the same time or after ROSS-DFT was developed.[12] Frank and co-workers[59] constructed a functional completely within the framework of DFT expressions. Their approach is based on a sum formula correction of UDFT energies (see, *e.g.* ref. 60); however, instead of doing two independent calculations for the OSS and the T state, these authors construct a total-energy functional for the OSS state in the spirit of the sum formula approach and minimize this functional with one set of KS orbitals. Filatov and Shaik[61] presented a similar but more general approach that can be extended to any low-spin open-shell state. Based on the generalization of DFT to fractional occupation numbers,[62] the same authors developed another method[63] that is appropriate for both type-I and certain type-II systems. Borowski and co-workers[64] investigated a number of two-configuration (TC)-SCF-based methods that aim at a description of type-II systems but treat the exchange and correlation energy for the two unpaired electrons in quite a similar fashion as the ROSS-DFT method. Wu and Shaik[65] recently presented a valence-bond (VB)-DFT approach, which is similar to the methods proposed in ref. 64. We note in this connection that the combination of TC methods such as GVB with DFT was explored and successfully applied already by Kraka and co-workers in 1991.[66]

In the case of type-III systems ROSS-DFT may still work reasonably; however, its spin-restricted character suppresses spin-polarization effects in the space of the doubly occupied orbitals, which can lead to an incorrect S–T energy ordering. In this case it is better to apply CAS-DFT, which combines a CASSCF description of static correlation effects with a coverage of dynamic correlation effects by a DFT correlation-energy functional. Due to the flexibility in choosing the active space, CAS-DFT can be applied to any multi-reference situation and is thus more flexible than ROSS-DFT. The numerical expenses of a CAS-DFT calculation are comparable to those of a CASSCF procedure, *i.e.* the calculation of the DFT contribution requires only a small part of the total computation time. The crucial part in constructing such a hybrid method is to cleanly separate the energy contributions to be covered by each of the approaches. In the CAS-DFT approach discussed in this work this was solved by a refinement of the method proposed by Savin[46] and Miehlich and co-workers.[47] First applications indicate that CAS-DFT describes both static and dynamic correlation effects in a reasonable way. They confirm the necessity of properly avoiding a double-counting of dynamic correlation effects, but also reveal that improvements have to be made for a balanced description of closed- and open-shell systems. A solution of the latter problem will be important to make CAS-DFT a routine method for future applications.[67]

Concerning the question posed in the title of this report we have provided evidence that DFT in form of a CAS-DFT approach can describe multi-reference problems as reliable as KS DFT describes closed shell molecules. Clearly, the XC functional has to be improved to increase the reliability of DFT results in general, but this does not contradict our basic conclusion as to the use of DFT in the case of multi-reference systems.

5. Acknowledgements

This work was supported by the Swedish Natural Science Research Council (NFR). All calculations were done on the CRAY C90 of the Nationellt Superdatorcentrum (NSC), Linköping, Sweden. The authors thank the NSC for a generous allotment of computer time.

References

1 (*a*) R. Shepard, in *Ab Initio Methods in Quantum Chemistry*, Part II, ed. K. P. Lawley, Advances in Chemical Physics, Wiley-Interscience, Chichester, 1987, vol. 69, p. 63; (*b*) B. O. Roos, in *Ab Initio Methods in Quantum Chemistry*, Part II, ed. K. P. Lawley, Advances in Chemical Physics 69, Wiley-Interscience, Chichester, 1987, p. 399.
2 R. J. Gdanitz and R. Ahlrichs, *Chem. Phys. Lett.*, 1988, **143**, 413.
3 H.-J. Werner, in *Ab Initio Methods in Quantum Chemistry*, Part II, ed. K. P. Lawley, Advances in Chemical Physics, Wiley-Interscience, Chichester, 1988, vol. 69, p. 1.
4 P. G. Szalay, in *Modern Ideas in Coupled-Cluster Methods*, ed. R. J. Bartlett, World Scientific, Singapore, 1997, p. 81.
5 K. Andersson and B. O. Roos, in *Modern Electron Structure Theory*, ed. R. Yarkony, Advanced Series in Physical Chemistry, Part I, World Scientific, Singapore, 1995, vol. 2, p. 55.
6 K. Wolinski, H. L. Sellers and P. Pulay, *Chem. Phys. Lett.*, 1987, **140**, 225.
7 P. Hohenberg and W. Kohn, *Phys. Rev. B*, 1964, **136**, B864.
8 W. Kohn and L. J. Sham, *Phys. Rev. A*, 1964, **140**, A1133.
9 J. Harris, *Phys. Rev. A*, 1984, **29**, 1648.
10 U. v. Barth, *Phys. Rev. A*, 1979, **20**, 1693.
11 H. Englisch and R. Englisch, *Phys. A*, 1983, **121A**, 253.
12 J. Gräfenstein, E. Kraka and D. Cremer, *Chem. Phys. Lett.*, 1998, **288**, 593.
13 C. C. J. Roothaan, *Rev. Mod. Phys.*, 1960, **32**, 179.
14 J. A. Pople, P. M. W. Gill and N. C. Handy, *Int. J. Quantum Chem.*, 1995, **56**, 80.
15 A. D. Becke, *J. Chem. Phys.*, 1993, **98**, 5648.
16 C. Lee, W. Yang and R. P. Parr, *Phys. Rev. B*, 1988, **37**, 785.
17 T. H. Dunning Jr, *J. Chem. Phys.*, 1989, **90**, 1007.
18 P. C. Hariharan and J. A. Pople, *Theor. Chim. Acta*, 1973, **28**, 213.
19 R. Krishnan, M. Frisch and J. A. Pople, *Chem. Phys.*, 1980, **72**, 4244.
20 E. Kraka, J. Gräfenstein, J. Gauss, F. Reichel, L. Olsson, Z. Konkoli, Z. He and D. Cremer, COLOGNE 99, Göteborg University, Göteborg, 1999.
21 M. J. Frisch, G. W. Trucks, H. B. Schlegel, G. E. Scuseria, M. A. Robb, J. R. Cheeseman, V. G. Zakrzewski, J. A. Montgomery Jr, R. E. Stratmann, J. C. Burant, S. Dapprich, J. M. Millam, A. D. Daniels, K. N. Kudin, M. C. Strain, O. Farkas, J. Tomasi, V. Barone, M. Cossi, M. R. Cammi, B. Mennucci, C. Pomelli, C. Adamo, S. Clifford, J. Ochterski, G. A. Petersson, P. Y. Ayala, Q. Cui, K. Morokuma, D. K. Malick, A. D. Rabuck, K. Raghavachari, J. B. Foresman, J. Cioslowski, J. V. Ortiz, B. B. Stefanov, G. Liu, A. Liashenko, P. Piskorz, I. Komaromi, R. Gomperts, R. L. Martin, D. J. Fox, T. Keith, M. A. Al-Laham, C. Y. Peng, A. Nanayakkara, C. Gonzalez, M. Challacombe, P. M. W. Gill, B. Johnson, W. Chen, M. W. Wong, J. J. Andres, M. Head-Gordon, E. S. Replogle and J. A. Pople, GAUSSIAN 98, Revision A.5, Gaussian, Inc., Pittsburgh PA, 1998.
22 M. H. Lim, S. E. Worthington, F. J. Dulles and C. J. Cramer, in *Chemical Applications of Density Functional Theory*, ACS Symposium Series, ed. B. B. Laird, R. B. Ross and T. Ziegler, American Chemical Society, Washington, DC, 1996, vol. 629, p. 402.
23 C. W. Bauschlicher, *Chem. Phys. Lett.*, 1980, **74**, 273.
24 J. S. Andrews, C. W. Murray and N. C. Handy, *Chem. Phys. Lett.*, 1993, **201**, 458.
25 (*a*) H. Petek, D. J. Nesbitt, D. C. Darwin, P. R. Ogilby, C. B. Moore and D. A. Ramsay, *J. Chem. Phys.*, 1989, **96**, 6566; (*b*) G. Herzberg, *Electronic Spectra of Polyatomic Molecules*, Van Nostrand Reinhold, New York, 1966.
26 A. R. W. McKellar, P. R. Bunker, T. J. Sears, K. M. Evenson, R. J. Saykally and S. R. Langhoff, *J. Chem. Phys.*, 1983, **79**, 5251.
27 H. F. Bettinger, P. v. R. Schleyer, P. R. Schreiner and H. F. Schaefer III, in *The Encyclopedia of Computational Chemistry*, ed. P. v. R. Schleyer, N. Allinger, T. Clark, J. Gasteiger, P. A. Kollman, H. F. Schaefer III and P. R. Schreiner, Wiley-Interscience, Chichester, 1998, p. 183.

28 C. W. Bauschlicher and S. R. Langhoff, *J. Chem. Phys.*, 1987, **87**, 387.
29 E. R. Davidson, in *Diradicals*, ed. W. T. Borden, Wiley-Interscience, New York, 1982, p. 73; N. C. Baird and K. F. Taylor, *J. Am. Chem. Soc.*, 1978, **100**, 1333; P. H. Mueller, N. G. Rondan, K. N. Houk, J. F. Harrison, D. Hooper, B. H. Willen and J. F. Liebman, *J. Am. Chem. Soc.*, 1981, **103**, 5049.
30 F. Bernardi, N. D. Epiotis, W. Cherry, H. B. Schlegel, M.-H. Whangbo and S. Wolfe, *J. Am. Chem. Soc.*, 1976, **98**, 469.
31 (*a*) E. A. Carter and W. A. Goddard, *J. Chem. Phys.*, 1988, **88**, 1752; (*b*) S. Khodabandeh and E. A. Carter, *J. Phys. Chem.*, 1993, **97**, 4360.
32 G. Xu, T.-M. Chang, J. Zhou and P. B. Shevlin, *J. Am. Chem. Soc.*, 1999, **121**, 7150.
33 D. Cremer and J. A. Pople, *J. Am. Chem. Soc.*, 1975, **97**, 1354; D. Cremer and K. J. Szabó, in *Methods in Stereochemical Analysis, Conformational Behavior of Six-Membered Rings, Analysis, Dynamics and Stereoelectronic Effects*, ed. E. Juaristi, VCH, New York, 1995, p. 59.
34 D. Cremer, E. Kraka, J. Gräfenstein, A. Hjerpe, Y. He, R. Wrobel and W. Sander, to be published.
35 NIST Standard Reference Database 25, Version 2.02, National Institute of Standards and Technology, Gaithersburg, MD, 1994.
36 J. Stanton and J. Gauss, *J. Chem. Phys.*, 1994, **101**, 3001.
37 K. M. Ervin, J. Ho and W. C. Lineberger, *J. Chem. Phys.*, 1989, **91**, 5974.
38 J. P. Perdew and A. Zunger, *Phys. Rev. B*, 1982, **23**, 5048.
39 J. Gräfenstein and D. Cremer, *Chem. Phys. Lett.*, 2000, **316**, 569.
40 J. P. Perdew, A. Savin and K. Burke, *Phys. Rev. A*, 1995, **51**, 4531.
41 G. C. Lie and E. Clementi, *J. Chem. Phys.*, 1974, **60**, 1275.
42 R. Colle and O. Salvetti, *Theor. Chim. Acta*, 1979, **53**, 55.
43 R. Colle and O. Salvetti, *J. Chem. Phys.*, 1990, **93**, 534.
44 (*a*) A. Savin and H.-J. Flad, *Int. J. Quantum Chem.*, 1995, **56**, 327; (*b*) T. Leininger, H. Stoll, H.-J. Werner and A. Savin, *Chem. Phys. Lett.*, 1997, **275**, 151.
45 (*a*) S. Grimme, *Chem. Phys. Lett.*, 1996, **259**, 128; (*b*) S. Grimme and M. Waletzke, *J. Chem. Phys.*, 1999, **111**, 5645.
46 A. Savin, *Int. J. Quantum Chem. Symp.*, 1988, **22**, 59.
47 B. Miehlich, H. Stoll and A. Savin, *Mol. Phys.*, 1997, **91**, 527.
48 M. Gell-Mann and K. Brueckner, *Phys. Rev.*, 1957, **106**, 364.
49 R. Colle and O. Salvetti, *Theor. Chim. Acta*, 1975, **37**, 329.
50 A. G. Myers and P. J. Proteau, *J. Am. Chem. Soc.*, 1989, **111**, 1146.
51 (*a*) A. G. Myers, P. S. Dragovich and E. Y. Kuo, *J. Am. Chem. Soc.*, 1992, **114**, 9369; (*b*) A. G. Myers and C. A. Parrish, *Bioconj. Chem.*, 1996, **7**, 322.
52 P. G. Wenthold, S. G. Wierschke, J. J. Nash and R. R. Squires, *J. Am. Chem. Soc.*, 1994, **116**, 7378.
53 J. Cabrero, N. Ben-Amor and R. Caballol, *J. Phys. Chem. A*, 1999, **103**, 6220.
54 P. G. Wenthold, S. G. Wierschke, J. J. Nash and R. R. Squires, *J. Am. Chem. Soc.*, 1993, **115**, 12611.
55 See, *e.g.*, K. Handrick, J. P. Malrieu and O. Castell, *J. Chem. Phys.*, 1993, **101**, 2205.
56 P. G. Wenthold, R. R. Squires and W. C. Lineberger, *J. Am. Chem. Soc.*, 1998, **120**, 5279.
57 J. Gräfenstein, A. M. Hjerpe, E. Kraka and D. Cremer, *J. Phys. Chem. A*, 2000, **104**, 1748.
58 S. G. Wierschke, J. J. Nash and R. R. Squires, *J. Am. Chem. Soc.*, 1993, **115**, 11958.
59 I. Frank, J. Hutter, D. Marx and M. Parrinello, *J. Chem. Phys.*, 1998, **108**, 4060.
60 T. Ziegler, A. Rauk and E. J. Baerends, *Theor. Chim. Acta*, 1977, **43**, 261.
61 M. Filatov and S. Shaik, *J. Chem. Phys.*, 1999, **110**, 116.
62 J. C. Slater, J. B. Mann, T. M. Wilson and J. H. Wood, *Phys. Rev.*, 1969, **184**, 672.
63 M. Filatov and S. Shaik, *Chem. Phys. Lett.*, 1999, **304**, 429.
64 P. Borowski, K. D. Jordan, J. Nichols and P. Nachtigall, *Theor. Chem. Acc.*, 1998, **99**, 135.
65 W. Wu and S. Shaik, *Chem. Phys. Lett.*, 1999, **301**, 37.
66 E. Kraka, D. Cremer and S. Nordholm, in *Molecules in Natural Science and Biomedicine*, ed. Z. B. Maksic and M. Eckert-Maksic, Ellis Horwood, Chichester, 1991, p. 351; E. Kraka, *Chem. Phys.*, 1992, **61**, 149.
67 J. Gräfenstein, to be published.